# Laser-Induced Periodical Structures Fabrication for Third Harmonic Generation

**T A Voytova, S V Makarov, A N Tsypkin, V A Milichko, I S Mukhin, A V Yulin, S E Putilin, M A Baranov, A E Krasnok, P A Belov**

ITMO University, 49 Kronverksky Pr., St. Petersburg, 197101, Russia

**Abstract**. We propose a novel strategy for self-adjusted fabrication of large-scale array of resonant silicon nanoparticles (metasurface) on a thin silicon film. The self-adjusting mechanism is based on the effect of resonant nanogratings formation under intense multishot femtosecond irradiation of a thin silicon film. The resulting metasurfaces allow for generation of ultraviolet laser pulses at a wavelength of 270 nm with conversion efficiency up to $10^{-6}$ and high peak (≈100 kW/sm$^2$) and average power (≈1.5μW). Such high peak power from ultrathin metasurface makes the generated UV pulses applicable in a wide range of applications: precise nanolithography, ultrafast photoexcitation etc.

## 1. Introduction

All-dielectric nanostructures and metasurfaces based on high refractive index dielectric nanoparticles have emerged as promising objects for nonlinear nanophotonics [1-3], competing with conventional dielectric microdevices [4]. Indeed, the low-loss all-dielectric nanoresonators, possessing electric and magnetic resonances in the visible range, provide efficient control of light scattering [5-9], strong light localization [10, 11], and effective wave front engineering [12], whereas nonlinear response of high-index dielectrics is very high [13]. For such high-intensity applications as optical harmonics generation from isotropic materials, e.g. silicon, it is important to have an effective thermal sink, in order to increase damage threshold and achieve higher output power of nonlinear signal. For this purpose, it is more reasonable to use homogeneous materials rather than nanoparticle-based metamaterials. Non-lithographical methods [14-17] imply formation of separate nanoparticles rather than surface nanostructuring preserving a good thermal contact with the remained film. On the other hand, femtosecond laser surface nanostructuring is proven to be high-efficient tool for fabrication of different single subwavelength nanoantennae [18-21], and for large-scale periodical surface nanostructuring [22-26]. In this paper, we apply self-organized laser-induced nanostructuring of thin *a*-Si:H film to fabricate array of periodically arranged nanoparticles (metasurface) placed on the homogeneous film, which provide resonance optical response at a pumping wavelength for enhanced third-harmonic generation (THG). The self-organized metasurfaces demonstrate up to 30-fold increase of the efficiency as compared with arbitrary nonresonant *a*-Si films and 2-fold improving as compared with an initial film supporting a Fabry-Perot resonance.

## 2. Samples fabrication

In order to enhance TH, we fabricate metasurface by irradiation of *a*-Si film with the thickness (100 nm) corresponding to the most effective THG. *a*-Si:H films with thicknesses were deposited on a substrate of fused silica by plasma enhanced chemical vapor deposition from $SiH_3$ precursor gas (initial hydrogen concentration ~10%), were used. The film irradiation is carried out by focusing of fs-laser pulses (100 fs) into 0.9 μm spot at 1/e level through a NA=0.75 objective. Surface scanning by

the focused beam with 0.1 J/cm2, repetition rate 10 kHz, and scan speed 20 μm/s provides ≈450 absorbed laser pulses per spot. The resulting metasurface represents periodical array of nanobumps with mean periods ≈260 nm along one axis and ≈700 nm along the perpendicular axis, the width of the bumps is ≈130 nm and the length is ≈330 nm (figure 1a). The 700-nm period is equal to scanning period of the laser nanostructuring. The all dimensions of the metasurface are smaller than the wavelength of fs-laser (800 nm) and all visible spectrum. Therefore, the structure can be considered as metasurface. Optimization of surface nanostructuring is represented in figure 2.

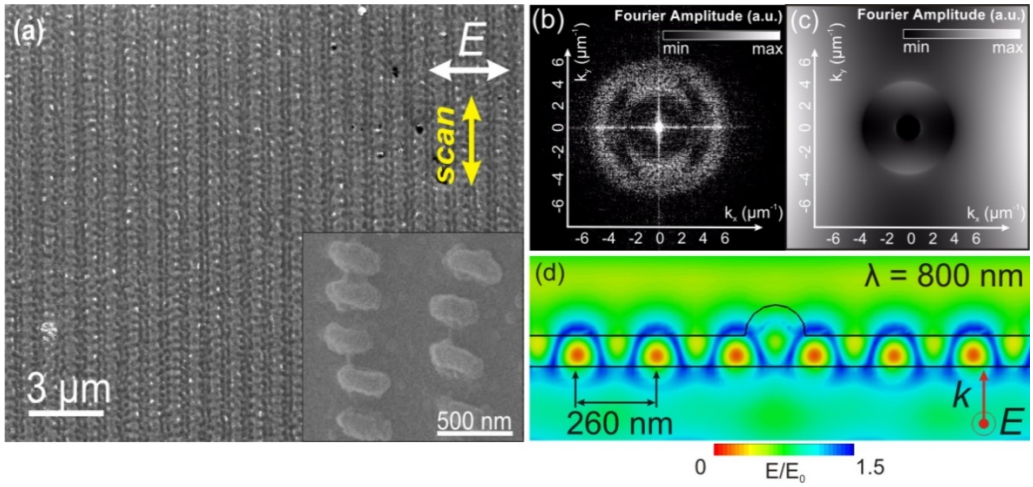


**Figure 1.** (a) SEM image of self-organized nc-Si metasurface. Inset: zoomed part of the metasurface. Experimental (b) and theoretical (c) spatial 2D Fourier spectra of the fabricated metasurface. (d) Calculated value of total electric field (averaged over time) near subwavelength hemispherical feature on 100-nm *a*-Si film after incidence of a plane electromagnetic wave.

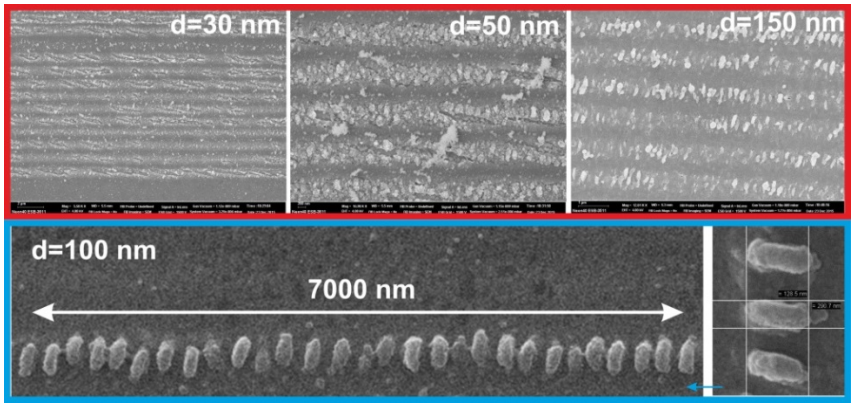


**Figure 2.** SEM images of nanostructured films by femtosecond laser irradiation with different thicknesses $d$.

### 3. Model for laser-induced metasurface formation

The most widely accepted theory of laser-induced periodical surface structures (LIPSS) is based on the interference of the incident laser beam with some form of a surface-scattered electromagnetic wave. The work of Sipe et al. [27] represents a first-principle theory which takes into consideration the interaction of an electromagnetic wave with a microscopically rough surface. This theory predicts possible LIPSS wave vectors $\mathbf{k}$ of the surface [with $|\mathbf{k}| = 2\pi/\Lambda$] as a function of the laser parameters angle of incidence $\theta$, polarization direction, and wave vector of the incident radiation $\boldsymbol{k_L}$ (with $|\mathbf{k_L}| = 2\pi/\lambda$) which has a component $\mathbf{k}_i$ in the surface plane and surface parameters (dielectric constant and surface roughness). It leads to an expression for the inhomogeneous energy deposition into the irradiated material which is proportional to $\eta(\mathbf{k}, \mathbf{k}_i) \times |b|$, where $\eta$ is a response function

describing the efficacy with which the surface roughness at **k** leads to inhomogeneous absorption of radiation. The second factor $b$ represents a measure of amplitude of the surface roughness at **k** which is a slowly varying function for a surface with a homogeneously distributed roughness. In contrast to the behavior of $b$, the efficacy factor $\eta$ can exhibit sharp peaks at certain **k** values which then determine the spatial ripple periods. It worth noting that once the LIPSS are formed, the Fourier spectrum of the surface $b(\mathbf{k})$ can also exhibit sharp peaks coincident with the peaks in $\eta(\mathbf{k})$ which were initially responsible for the surface damage.

In the theory of Sipe et al., the efficacy factor is defined as $\eta(\mathbf{k}, \mathbf{k}_i) = 2\pi|\nu(\mathbf{k}_+) + \nu^*(\mathbf{k}_-)|$. For the two cases of s- or p-polarized light, incident under an angle of $\theta$ and having polarization vectors and a wave vector component $\mathbf{k}_i$ the complex function $\nu$ is given by

$$\nu(\mathbf{k}_\pm, \mathrm{s-pol.}) = \left[h_{ss}(k_\pm)\left(\hat{\mathbf{k}} \pm \cdot\, \hat{\mathbf{y}}\right)^2 + h_{kk}(k_\pm)\left(\hat{\mathbf{k}} \pm \cdot\, \hat{\mathbf{x}}\right)^2\right]\gamma_t |t_s(\mathbf{k}_i)|^2, \quad (1)$$

$$\begin{aligned}\nu(\mathbf{k}_\pm, \mathrm{p-pol.}) = &\left[h_{ss}(k_\pm)\left(\hat{\mathbf{k}} \pm \cdot\, \hat{\mathbf{x}}\right)^2 + h_{kk}(k_\pm)\left(\hat{\mathbf{k}} \pm \cdot\, \hat{\mathbf{y}}\right)^2\right]\gamma_t |t_s(\mathbf{k}_i)|^2 + \\ &h_{kz}(k_\pm)\left(\hat{\mathbf{k}} \pm \cdot\, \hat{\mathbf{y}}\right)\gamma_z \varepsilon t_x^*(\mathbf{k}_i) t_z(\mathbf{k}_i) + h_{zk}(k_\pm)\left(\hat{\mathbf{k}} \pm \cdot\, \hat{\mathbf{y}}\right)\gamma_t t_x(k_i) t_z^*(\mathbf{k}_i) + \\ &h_{zz}(k_\pm)\gamma_z \varepsilon |t_z(\mathbf{k}_i)|^2, \end{aligned} \quad (2)$$

with inner products $\left(\hat{\mathbf{k}} \pm \cdot\, \hat{\mathbf{y}}\right) = (\sin\theta \pm \kappa_y)/\kappa_\pm$ and $\left(\hat{\mathbf{k}} \pm \cdot\, \hat{\mathbf{x}}\right) = \kappa_x/\kappa_\pm$. Here, the definition $\kappa_\pm = [\kappa x^2 + (\sin\theta \pm k_y)^2]^{1/2}$ has been used and all lengths have been normalized with the factor $\lambda/(2\pi)$. Hence, the dimensionless LIPSS wave vectors $\kappa = k \cdot \lambda(2\pi) \equiv \lambda/\Lambda$ are used in the following. With these definitions and with $\varepsilon$ being the complex dielectric function of the material at the irradiation wavelength, the functions $h_{ss}$, $h_{zz}$, $h_{kk}$, $h_{kz}$, $h_{zk}$ used in equations (2) and (3) can be expressed as

$$h_{ss}(k_\pm) = 2i\left(\sqrt{1-\kappa_\pm^2} + \sqrt{\varepsilon - \kappa_\pm^2}\right)^{-1}, \quad h_{zz}(k_\pm) = 2i\kappa_\pm^2\left(\sqrt{1-\kappa_\pm^2} + \sqrt{\varepsilon - \kappa_\pm^2}\right)^{-1}, \quad (3)$$

$$h_{kk}(k_\pm) = \frac{2i}{\varepsilon}\sqrt{(\varepsilon - \kappa_\pm^2)(1-\kappa_\pm^2)}\left(\sqrt{1-\kappa_\pm^2} + \sqrt{\varepsilon - \kappa_\pm^2}\right)^{-1}, \quad (4)$$

$$h_{kz}(k_\pm) = \frac{2i\kappa_\pm}{\varepsilon}\sqrt{(\varepsilon - \kappa_\pm^2)}\left(\sqrt{1-\kappa_\pm^2} + \sqrt{\varepsilon - \kappa_\pm^2}\right)^{-1}, \quad (5)$$

$$h_{zk}(k_\pm) = \frac{2i\kappa_\pm}{\varepsilon}\sqrt{(1 - \kappa_\pm^2)}\left(\sqrt{1-\kappa_\pm^2} + \sqrt{\varepsilon - \kappa_\pm^2}\right)^{-1}. \quad (6)$$

The complex functions $t_s$, $t_z$, and $t_x$ are given by

$$t_s(\mathbf{k}_i) = 2|\cos\theta|\left(|\cos\theta| + \sqrt{\varepsilon - (\sin\theta)^2}\right)^{-1}, \quad t_z(\mathbf{k}_i) = 2\sin\theta\left(\varepsilon|\cos\theta| + \sqrt{\varepsilon - (\sin\theta)^2}\right)^{-1}, \quad (7)$$

$$t_x(\mathbf{k}_i) = 2\sqrt{\varepsilon - (\sin\theta)^2}\left(\varepsilon|\cos\theta| + \sqrt{\varepsilon - (\sin\theta)^2}\right)^{-1}. \quad (8)$$

The surface roughness is included in the theory in the factors $\gamma_t$ and $\gamma_z$ via two numerical factors, $s$ (shape factor) and $f$ (filling factor), by

$$\gamma_t = \frac{\varepsilon - 1}{4\pi(1 + 0.5(1-f)(\varepsilon-1)(F(s) - R \cdot G(s)))}, \quad \gamma_z = \frac{\varepsilon - 1}{4\pi(\varepsilon - (1-f)(\varepsilon-1)(F(s) + R \cdot G(s)))}, \quad (9)$$

with $R = (\varepsilon - 1)/(\varepsilon + 1)$ and the scalar functions $F(s) = \sqrt{s^2 + 1} - s$ and $Q(s) = 0.5\left(\sqrt{s^2 + 4} + s\right) - \sqrt{s^2 + 1}$.

Following [27], the surface roughness was modeled with the values $s$=0.4, $f$=0.1, which represent the assumption of spherically shaped islands. On the basis of equations (1) - (9) it is possible to calculate numerically the efficacy factor $\eta$ as a function of the normalized LIPSS wave vector

components $\kappa_x$, $\kappa_y$ at given values for the irradiation parameters ($\theta$, $\lambda$ and polarization direction) and for parameters characterizing the optical ($\varepsilon$) and the surface roughness properties ($s$ and $f$). The calculated 2D Fourier spectrum of laser energy deposition (for real and imagine parts or complex refractive index, respectively, $n$=3.90 and $K$=0.11 at $\lambda$=800 nm [28]) exhibits pronounced maxima for structures with period around $\lambda/n \approx$205 nm and with wavevectors perpendicular to the laser polarization (figure 1b,c).

Despite excellent qualitative agreement, analytical modeling based on the widely acknowledged Sipe's model [27] does not provide quantitative prediction of the periods between nanoparticles within the metasurface, because it does not take into account film thickness. In numerical simulations we observe coupling of normally incident laser wave to a planar waveguide mode within the Si film. This coupled waveguide mode interferes with the incident field, providing the formation of a standing wave within the film and modulated heating with the period about 260 nm. Figure 1b supports the interference mechanism, where the scattering of the incident electromagnetic wave with 800 nm wavelength on a single subwavelength particle on Si 100-nm. The electric field enhancement within each maximum is about 1.5, resulting in ultrafast non uniform heating and deformation of the film due to thermal expansion and fast resolidification.

It is worth noting, that the surface plasmon-polaritons excitation [20, 24, 25] is unlikely to be the origin of the metasurface formation in our case, because the wavevector of the periodical arrays is perpendicular to polarization of the incident light (Fig.1a), whereas plasmon-polaritons are mostly longitudinal waves [29]. Moreover, quality of nanostructuring is the best for 100-nm film as compared to the other *a*-Si:H films, revealing an important role of the waveguiding mode.

## 4. Third harmonics generation from the nanostructure

For THG generation a commercial femtosecond laser system (based on a Ti:Sapphire regenerative amplifier Regulus 35F1K, Avesta Poject) was used. Laser pulses have 800 nm central wavelength, with maximum pulse energy of 2 mJ, and pulse duration of 40 fs at the repetition rate of 1 kHz. Laser energy was varied and controlled by an polarising filter and a power meter (Nova II, Ophir), respectively, while the pulse duration was measured by an autocorrelator ASF-20 (Avesta Poject). The THG signal was separated from the fundamental wavelength by a set of filters and measured by the power meter. Measured UV signal can be clearly seen by a spectrometer, excluding the influence of possible one-photon or multiphoton luminescence.

Importantly, a smooth Si film, supporting Fabry-Perot resonance at 800 nm and formation of resonant metasurface, shows a sharp maximum of UV signal at 100—120 nm thicknesses (figure 3a). The largest difference in THG signal is observed between 170-nm and 100-nm films, giving 15-fold enhancement [30]. In figure 3b the comparison of UV signal from the metasurface with UV signal from the thin 100-nm film is presented, revealing 2.5-fold enhancement of third-harmonics conversion efficiency and the 30-fold enhancement as compared to the nonresonant 170-nm film. The observed maximum TH conversion efficiency is about $0.9 \cdot 10^{-6}$ for the 100-nm film and incident pulse energy 1.5 mJ. In our experiments, maximum laser intensity is much smaller than the damage threshold of a Si film (100 mJ/cm$^2$) [17] and the level of dense electron-hole plasma generation ($F$=1 mJ/cm$^2$) [1, 2, 31, 32]. Despite the conversion efficiency for our system is not a record among previously reported values achieved in high-Q resonantors [4, 32], the measured output energies and average power of UV femtosecond laser pulses are much larger.

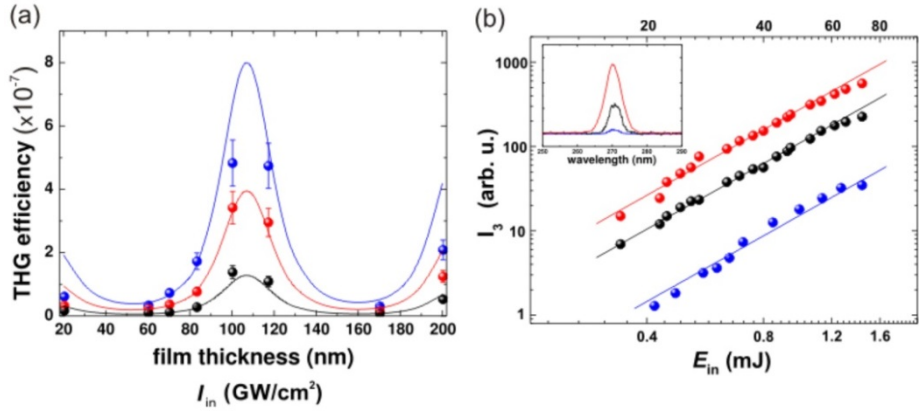


**Figure 3.** (a) Experimental (circles) and theoretical (lines) dependencies of third harmonic generation (THG) efficiency on Si film thickness at various pump intensities: 20 GW/cm$^2$ (black), 35 GW/cm$^2$ (red), 55 GW/cm$^2$ (blue). (b) Experimental dependencies of third harmonic intensity from initial (black dots) and nanostructured Si films with 100-nm thickness on fused silica substrate with resonant (red dots). Third harmonics signal from smooth 170-nm Si film (blue dots). All approximation lines correspond to 2.8 slope. Inset: spectral range in the vicinity of the third harmonic signal.

Indeed, the advantage of our systems is that they allow working with much more powerful pump and to generate UV femtosecond pulses with the energy as high as $W$=1.3 nJ per pulse. This value is at least 5 orders of magnitude higher than that reported and yields high average power of femtosecond UV beam about $P_{av}$==1.3 μW, being high enough to provide visible fluorescence of strontium aluminate doped with europium and dysprosium in quartz cuvette. The maximum estimated peak power of the UV pulse is up to $P_{peak}$~$10^5$ W at the $\lambda$ =270 nm. The shortest pulse duration $\tau_3$ of the UV pulse at such parameters is estimated to be 15 fs.

The experimental results can be described in terms of excitation of modes within a film or nanostructure. The intensity of the emitted third harmonic $I_3$ from the unit square of the surface can be expressed through the integral of the product of the Green function $G(x)$ and the nonlinear current $j_n(x)$ over film or nanostructure thickness $d$ as $I_3 \sim |E_3|^2 = \left|\int_0^d G(x) j_n(x) dx\right|^2$. In turn, the nonlinear current can be expressed as $j_n = \chi^{(3)} \cdot E_1^3$, where $E_1$ is electric field at the fundamental frequency and $\chi^{(3)}$ is nonlinear susceptibility. It is clearly seen that the efficiency of the third harmonics depends not only on the intensity distribution of the nonlinear current $j_n(x)$ but also on the Green function $G(x)$, which characterize resonances of the structure. Thus the resonances on the frequency of the third harmonics can also enhance the emission of the radiation. Figure 3a shows the dependencies of THG efficiency $\eta$ on the film thickness calculated using the Green function rigorously calculated for the planar structure. The fundamental field distribution cannot be found analytically for real geometry. However, for the experimental conditions the losses are high at the frequency of the third harmonic and thus only the radiation from a thin layer close to the interface is important.

## 5. Conclusion

In summary, we have applied self-organized laser-induced nanostructuring of thin Si film to fabricate all-dielectric metasurface, which provides resonance optical response at a pumping wavelength for third-harmonic generation. The proposed method is extremely convenient and fast, because one does not need to develop a specific design of a metasurface for the strongest field enhancement. The self-adjusted metasurface has demonstrated 2.5-fold improvement of THG as compared with an initial film with the highest conversion efficiency. This allows to achieve UV radiation at the wavelength 270 nm with high peak and average power ($10^5$ kW and 1.5 μW, correspondingly). Moreover, according to spectral width of the UV pulses, their duration could be as short as 15 fs.

**Acknowledgments**
This work was financially supported by Government of Russian Federation (RFMEFI58414X0009).

**References**
[1] Shcherbakov M R 2014 *Nano Letters* **14** 6488
[2] Makarov S, Kudryashov S, Mukhin I, Mozharov A, Milichko V, Krasnok A and Belov P 2015 *Nano Letters* **15** 6187
[3] Carletti L, Locatelli A, Stepanenko O, Leo G and De Angelis C 2015 *Opt. Express* **23** 26544
[4] Leuthold J, Koos C and Freude W 2010 *Nature Photonics* **4** 535
[5] Popa B-I and Cummer S A 2008 *Physical Review Letters* **100** 207401
[6] Zhao Q, Zhou J, Zhang F and Lippens D 2009 *Materials Today* **12** 60
[7] Evlyukhin A B, Reinhardt C, Seidel A, Lukyanchuk B S and Chichkov B N 2010 *Physical Review* B **82** 045404
[8] Garcia-Etxarri A, Gomez-Medina R, Froufe-Perez L S, Lopez C, Chantada L, Scheffold F, Aizpurua J, Nieto-Vesperinas M and Saenz J J 2011 *Opt. Express.* **19** 4815
[9] Miroshnichenko A E, Evlyukhin A B, Yu Y F, Bakker R M, Chipouline A, Kuznetsov A I, Lukyanchuk B, Chichkov B N and Kivshar Y S 2015 *Nature Communication* **6** 8069
[10] Bakker R M et al. 2015 *Nano Letters* **15** 2137
[11] Caldarola M, Albella P, Cortes E, Rahmani M, Roschuk T, Grinblat G, Oulton R F, Bragas A V, and Maier S A 2015 *Nature Communication* **6** 7915
[12] Decker M, Staude I, Falkner M, Dominguez J, Neshev D N, Brener I, Pertsch T and Kivshar Y S 2015 *Advanced Optical Materials* **3** 813
[13] Boyd R W 2003 *Nonlinear optics* (Academic Press)
[14] Shi L, Tuzer T U, Fenollosa R and Meseguer F 2012 *Advanced Materials* **24** 5934
[15] Moitra P, Slovick B A, Li W, Kravchenko I I, Briggs D P, Krishnamurthy S and Valentine J 2015 *ACS Photonics* **2** 692
[16] Abbarchi M et al. 2014 *ACS Nano* **6** 11181
[17] Dmitriev P, Makarov S V, Milichko V, Mukhin I, Gudovskikh A, Sitnikova A, Samusev A, Krasnok A and Belov P 2015 *Nanoscale* **8** 5043
[18] Kuznetsov A I, Evlyukhin A B, Goncalves M R, Reinhardt C, Koroleva A, Arnedillo M L, Kiyan R, Marti O and Chichkov B N 2011 *ACS Nano* **5** 4843
[19] Reininghaus M, Wortmann D, Cao Z, Hoffmann J M and Taubner T 2013 *Opt. Express* **21** 32176
[20] Kuchmizhak A, Ionin A, Kudryashov S, Makarov S, Rudenko A, Kulchin Y N, Vitrik O and Efimov T 2015 *Opt. Lett.* **40** 1678
[21] Makarov S V, Milichko V A, Mukhin I S, Shishkin I I, Zuev D A, Mozharov A M, Krasnok A E and Belov P A 2014 *Laser Photonics Reviews* **10** 91
[22] Le Harzic R, Schuck H, Sauer D, Anhut T, Riemann I and Konig K 2005 *Opt. Expess* **13** 6651
[23] Tang M, Zhang H and Her T-H 2007 *Nanotechnology* **18** 485304
[24] Huang M, Zhao F, Cheng Y, Xu N and Xu Z 2009 *ACS Nano* **3** 4062
[25] Bonse J, Rosenfeld A and Kruger J 2009 *Journal of Applied Physics* **106** 104910
[26] Vorobyev A, Makin V and Guo C 2009 *Physical Review Letters* **102** 234301
[27] Sipe J, Young J F, Preston J and Van Driel H 1983 *Physical Review* B **27** 1141
[28] Palik E D 1998 *Handbook of optical constants of solids* (Academic Press)
[29] Raether H 1998 *Surface plasmons on smooth surfaces* (Springer)
[30] Saeta P N and Miller N 2001 *Applied Physics Letters* **79** 2704
[31] Shcherbakov M R et al. 2015 *Nano Letters* **15** 6985
[32] Yang Y, Wang W, Boulesbaa A, Kravchenko I I, Briggs D P, Puretzky A, Geohegan D and Valentine J 2015 *Nano Letters* **15** 7388